Infrared Absorption of Liquid and Solid Hydrogen with Various Ortho-Para Ratios*

W. F. J. HARE,† ELIZABETH J. ALLIN, AND H. L. WELSH
McLennan Laboratory, University of Toronto, Toronto, Canada
(Received July 21, 1955)

THE fundamental vibrational absorption of liquid and solid normal hydrogen has recently been studied in the temperature range, 10–22°K.[1] These experiments, designed to show the transition from collision-induced absorption in the high-pressure gas[2] to the corresponding phenomena in the condensed phases, have now been extended to various mixtures of ortho- and parahydrogen. Parahydrogen, prepared by the method described by Squires and Stewart,[3] was mixed with normal hydrogen at room temperature and the mixture condensed in the absorption cell previously described.[1]

Absorption profiles for solid hydrogen, 8.4 mm thick, with different ortho-para ratios are shown in Fig. 1. Three groups of main maxima are apparent: the Q group (Q_Q,Q_R) near the band origin, the $S(0)$ group [$S_1(0)$,$S_2(0)$,$S'(0)$] corresponding to the *para*-transition $J=0\rightarrow J=2$, and the $S(1)$ group [$S_1(1)$,$S_2(1)$, $S'(1)$] corresponding to the *ortho*-transition $J=1\rightarrow J=3$. The weak component, $S_2(0)$, is clearly resolved only in pure parahydrogen. The maxima designated as $2S(0)$, $S(0)+S(1)$, and $2S(1)$ are due to double rotational transitions; in parahydrogen only $2S(0)$ remains.

The broad components Q_R, $S'(0)$ and $S'(1)$ are clearly summation tones of the molecular vibrational and rotational frequencies with the vibrational frequencies of the crystal lattice. The shapes of these components are independent of, and their intensities vary linearly with the ortho-para ratio; thus, the transition probabilities (intensity/ortho or para concentration) are independent of the ortho-para ratio. The Q_R component can be separated into para and ortho contributions, and the transition probabilities are in the proportion $Q_R(\text{para}):Q_R(\text{ortho}):S'(0):S'(1)=10:19:22:11$. The Q_R component has its analog in the spectrum of the high pressure gas where it is interpreted as a "summation tone" of the vibrational frequency of the absorbing molecule with the relative kinetic energy of the colliding molecule and of the surrounding molecules; for this type of absorption close collisions, in the region of overlap forces, appear to be necessary.[2]

The intensities of the strong sharp lines Q_Q, $S_1(0)$ and $S_1(1)$ vary in a complex manner with the ortho-para ratio. In parahydrogen the Q_Q component has zero intensity, showing that the transition $J=0\rightarrow J=0$ is forbidden. When the intensities are corrected for overlapping with other components, and when the data for the Q_Q and $S(1)$ components are extrapolated, the transition probabilities for parahydrogen are approximately in the proportion $Q_Q:S_1(0):S_1(1)=6:5:9$. In the theory of van Kranendonk and Bird the transition probabilities for rotation-vibrational transitions induced by quadrupole interaction are given by $\times 3(J+1)(J+2)/2(2J+3)$ for $\Delta J=+2$ and $J(J+1)(2J+1)/(2J-1)(2J+3)$ for $\Delta J=0$. Since the observations in parahydrogen are in accordance with these it is concluded that the Q_Q, $S_1(0)$ and $S_1(1)$ components arise from quadrupole interaction. However, when the ortho-para ratio is not zero the observed relative transition probabilities differ widely from those given by the theoretical expressions. When the probabilities are extrapolated for the case of orthohydrogen they are in the proportion $Q_Q:S_1(0):S_1(1)=6:32:9$. The quadrupole effect thus seems to depend on whether the molecules in the neighborhood of the absorbing molecule are rotating or nonrotating.

The weak sharp lines $S_2(0)$ and $S_2(1)$ have the same frequency separation as the corresponding lines in the Raman effect of the gas[4]; for these, unlike the other components of the band, the B value is unperturbed. These lines may be due to the average quadrupole effect in the solid. The much stronger quadrupole effect giving rise to the Q_Q, $S_1(0)$ and $S_1(1)$ lines may perhaps be construed as a special two-body "encounter"

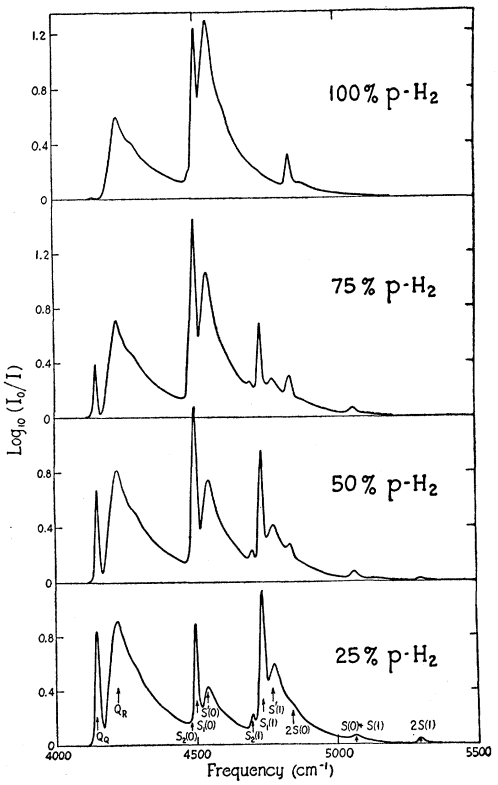

FIG. 1. The variation with ortho-para ratio of the fundamental infrared absorption of solid hydrogen at a temperature of 13.6±0.2°K.

of the absorbing molecule with one of its nearest neighbors, distinguished by the relative orientation of the quadrupole moments of the two molecules. These conclusions must be regarded as tentative.

* This research was supported by a grant from the National Research Council of Canada.

† Holder of a Research Fellowship of the National Research Council of Canada.

[1] Allin, Hare, and MacDonald, Phys. Rev. **98**, 554 (1955).
[2] D. A. Chisholm and H. L. Welsh, Can. J. Phys. **32**, 391 (1954).
[3] G. L. Squires and A. T. Stewart, J. Chem. Phys. **22**, 754 (1954).
[4] C. Cumming, Ph.D. thesis, University of Toronto, 1952 (unpublished).

Electron Traps in Silver Chloride

HIROSHI KANZAKI
Institute of Industrial Science, University of Tokyo, Chiba, Japan
(Received June 22, 1955)

EXPERIMENTAL evidence[1] is now available for trapping of electrons at dislocations in AgCl crystals. Seitz[2] proposed that the traps are incipient vacancies with an effective charge of $+e/2$, and his prediction has received further support in the work of Hedges and Mitchell[3] who have found that the silver particles produced by light outline the polygonized substructure in AgBr crystals.

The writer wishes to propose that the electron traps in well-annealed crystals of AgCl are: (a) the kink sites at the surface, (b) the emergence points of edge dislocations at the surface, and (c) the nodes in the dislocation networks inside the crystal. This proposal stems from the observation of print-out silver in well-annealed crystals of AgCl and some of the results will be described here.

In crystals with the surface parallel to (111),[4] two kinds of silver particles are observed at the surface (Fig. 1). They are: (1) the larger particles which outline the hexagonal pattern and are supposed to have been produced at the (b) sites described above, and (2) the smaller particles which are distributed around the hexagonal pattern and probably have been produced at the (a) sites.

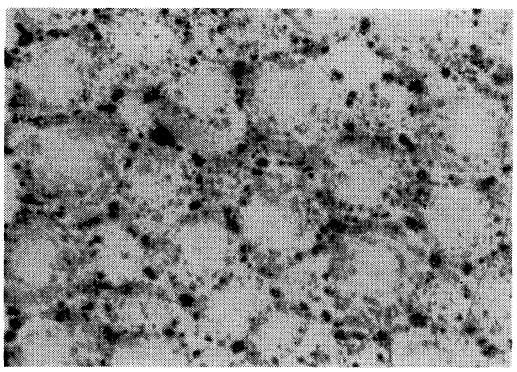

FIG. 1. Print-out silver particles at the surface of a AgCl crystal with (111) surface (×600).

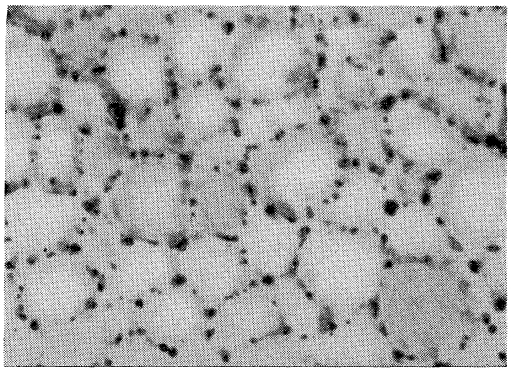

FIG. 2. Print-out silver particles inside the AgCl crystal with (111) surface (×600).

In the interior, the particles are distributed discontinuously upon the hexagonal cylindrical surfaces outlined by the particles of (1) at the surface (Fig. 2) and are supposed to have been produced at the nodes of dislocation networks extended on the cylindrical surfaces.

This selective production of silver particles may be explained by the trapping of electrons by effective charges. In the case of traps at the (b) sites, the extra (110) half-plane accompanied by the edge components of dislocations may produce extra charge by intersecting (111) and (100) surface planes, but cannot do this at the (110) surface plane. This prediction has been confirmed by the following experiments.

Figure 3 shows the distribution of silver particles near the grain boundary. The right-hand grain with (100) surface has been subjected to extensive darkening and the left-hand one with (110) surface has produced very little silver. Chemical etching[5] revealed etch pits due to dislocations (probably with edge components) in the (110) grain but not in the (100) grain. Figure 4 shows the etching pattern near the grain boundary of

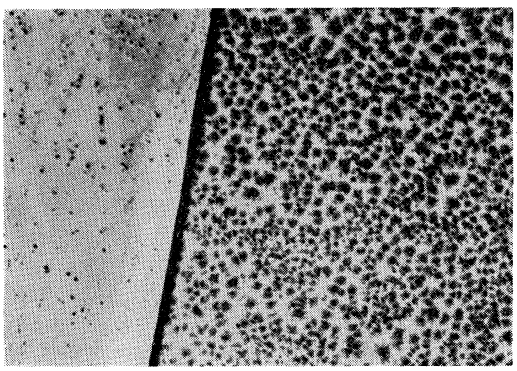

FIG. 3. Print-out silver particles near the grain boundary. The right-hand crystal has a (100) surface and the left-hand crystal has a (110) surface (×320).